View metadata, citation and similar papers at core.ac.uk

brought to you by CORE

provided by Carolina Digital Repository

click for updates

SEE COMMEN

Chemical shift imprint of intersubunit communication in a symmetric homodimer

Bradley T. Falk[a], Paul J. Sapienza[b], and Andrew L. Lee[a,b,1]

[a]Department of Biochemistry and Biophysics, School of Medicine, University of North Carolina at Chapel Hill, Chapel Hill, NC 27599; and [b]Division of Chemical Biology and Medicinal Chemistry, UNC Eshelman School of Pharmacy, University of North Carolina at Chapel Hill, Chapel Hill, NC 27599

Edited by Adriaan Bax, National Institutes of Health, Bethesda, MD, and approved June 21, 2016 (received for review March 24, 2016)

Allosteric communication is critical for protein function and cellular homeostasis, and it can be exploited as a strategy for drug design. However, unlike many protein–ligand interactions, the structural basis for the long-range communication that underlies allostery is not well understood. This lack of understanding is most evident in the case of classical allostery, in which a binding event in one protomer is sensed by a second symmetric protomer. A primary reason why study of interdomain signaling is challenging in oligomeric proteins is the difficulty in characterizing intermediate, singly bound species. Here, we use an NMR approach to isolate and characterize a singly ligated state ("lig$_1$") of a homodimeric enzyme that is otherwise obscured by rapid exchange with apo and saturated forms. Mixed labeled dimers were prepared that simultaneously permit full population of the lig$_1$ state and isotopic labeling of either protomer. Direct visualization of peaks from lig$_1$ yielded site-specific ligand-state multiplets that provide a convenient format for assessing mechanisms of intersubunit communication from a variety of NMR measurements. We demonstrate this approach on thymidylate synthase from *Escherichia coli*, a homodimeric enzyme known to be half-the-sites reactive. Resolving the dUMP$_1$ state shows that active site communication occurs not upon the first dUMP binding, but upon the second. Surprisingly, for many sites, dUMP$_1$ peaks are found beyond the limits set by apo and dUMP$_2$ peaks, indicating that binding the first dUMP pushes the enzyme ensemble to further conformational extremes than the apo or saturated forms. The approach used here should be generally applicable to homodimers.

homodimer | subunit communication | allostery | NMR | thymidylate synthase

Allosteric regulation in proteins is a ubiquitous mechanism for controlling cellular behavior and an attractive strategy for therapeutic development. Even though broadly recognized, long-range communication is not well understood mechanistically (1–4). Although there have been numerous strategies to reveal the structural and dynamic underpinnings of allostery, oddly these strategies have largely focused on complex oligomeric or, alternatively, on small monomeric allosteric proteins. A likely more straightforward approach is to study allosteric mechanisms using simple symmetric homodimeric proteins, which would allow for answering the basic and general question of how the occurrence of an event in one subunit is communicated to another subunit, as occurs in classical multisubunit allosteric proteins. Given the large number of homodimeric proteins involved in cellular regulation (such as growth factors, cytokines, kinases, G protein-coupled receptors, transcription factors, and metabolic proteins), insights into intersubunit communication should be widely beneficial (5).

As a key step toward a broad understanding of allosteric mechanisms, it will be important to observe how binding a ligand in one subunit is communicated to a second subunit, even in the absence of conformational change. Although this communication is straightforward in specific cases of two differing neighboring domains or heterodimers in which domains have distinct ligands (6–8), it is more elusive for the common case of symmetric homodimers. Homodimers present a challenge because it is difficult to either observe individual protomers or study states with a single ligand bound (referred to here as "lig$_1$") because of dynamic binding equilibria. Having a method to isolate lig$_1$ homodimers would facilitate detailed study of intersubunit communication and allostery by high resolution structural methods. A well-established approach for mapping communication networks in proteins is NMR spectroscopy, most commonly using so-called chemical shift perturbation (CSP) (9, 10). In the case of homodimers, however, tracking CSPs or making additional measurements on lig$_1$ peaks (or resonances) becomes problematic because (*i*) resonances from symmetric protomers can overlap, (*ii*) resonances are frequently in fast or intermediate exchange on the NMR timescale, especially in dimeric enzymes where substrate affinities are low to moderate, and, most importantly, (*iii*) unless ligand binding is highly negatively cooperative, there will be additional resonances from apo (lig$_0$) and doubly bound (lig$_2$) states. In principle, monitoring lig$_1$ states is most easily carried out in highly negatively cooperative systems although, even in the few reported cases, most lig$_1$ resonances were not well resolved (11, 12). A general, experimental format for monitoring specific peaks (or sites) in both bound and empty protomers for lig$_1$ states will therefore help advance our understanding of intersubunit communication and allostery in homodimers (and potentially higher order oligomers).

Escherichia coli thymidylate synthase (TS), a 62-kDa symmetric homodimer, presents a favorable example for lig$_1$ studies by NMR. TS catalyzes the synthesis of the sole source of 2′-deoxythymidine-5′-monophosphate (dTMP) via a multistep mechanism involving reductive methylation of dUMP using N5,N10-methylene-5,6,7,8-tetrahydrofolate (mTHF) as both a methylene and hydride donor. In addition, TS is half-the-sites reactive (13–15), with substrate binding sites separated by 35 Å, leading to an expectation for

Significance

Regulatory signals between protein subunits depend on communication between sequential binding events. How such long-range communication, or allostery, operates at the subdomain level has been elusive, especially for homooligomeric proteins. To address this problem, homodimers of thymidylate synthase were generated for optimized study of individual protomers of the singly bound dimer. Mixed ^{15}N-labeled dimers were created with a single functional active site, allowing site-specific, protomer-specific chemical shifts to report on step-wise binding effects. Long-range intersubunit communication was observed although this communication was apparent only in the second ligand-binding step, in which changes were in the first ligand-bound region. Visualization of up to four peaks for each residue amide provides a unique way to assess the allosteric mechanism.

Author contributions: B.T.F., P.J.S., and A.L.L. designed research; B.T.F. and P.J.S. performed research; B.T.F., P.J.S., and A.L.L. analyzed data; and B.T.F., P.J.S., and A.L.L. wrote the paper.

The authors declare no conflict of interest.

This article is a PNAS Direct Submission.

See Commentary on page 9407.

[1]To whom correspondence should be addressed. Email: drewlee@unc.edu.

This article contains supporting information online at www.pnas.org/lookup/suppl/doi:10.1073/pnas.1604748113/-/DCSupplemental.

negative substrate binding cooperativity between protomers. Although dUMP was recently shown to bind with minimal cooperativity for the *E. coli* enzyme at 25 °C, there are signs of unequal thermodynamics between the two protomers at lower temperatures (16), and indeed data herein show clear intersubunit communication. Moreover, other TS enzymes, and in particular human, seem to show more dramatic cooperativity, suggesting that intersubunit communication is an intrinsic feature of TS (13, 17–21). To overcome the difficulties of studying symmetric proteins by NMR, we generated a pair of mixed labeled dimers of TS that each have a single functional active site and a single protomer labeled for NMR studies. These complementary mixed dimers allow for determining protomer-specific responses to a single dUMP binding event by isolating the $dUMP_1$ state. In the presence of dUMP, the mixed dimers revealed $dUMP_1$ peak positions normally hidden in WT (wild-type) dimer titrations and highlighted the important differences between the two dUMP binding events. These data also allow construction of complete "ligand state peak multiplets" that reflect the responses of residues on both sides of the interface. Most notably, we show that there is communication between the two active sites primarily upon binding the second dUMP because this binding event causes perturbations in the already-bound first site.

Materials and Methods

Protein Expression and Purification. WT and double mutant R126E, R127E (RREE) thymidylate synthase from *E. coli* was expressed and purified as described in *SI Materials and Methods*.

Generation of TS Mixed Dimers. Preparation of specific labeled mixed dimers was accomplished in vitro by mixing purified WT and RREE homodimers, in 2 M urea at pH 9, to reapportion the monomers yielding three species: WT and RREE homodimers and a mixed dimer with one WT and one RREE monomer. The mixed dimer was then separated from the parent homodimers by anion exchange chromatography. For NMR studies, two different preparations of mixing were made to isolate both species of mixed dimers: one where the binding subunit is U-[^{2}H, ^{15}N]–labeled (mix RREE-labeled with WT-unlabeled) and one where the nonbinding subunit is U-[^{2}H, ^{15}N]–labeled (mix WT-labeled with RREE-unlabeled). For full details, see *SI Materials and Methods*.

NMR Spectroscopy. Standard transverse relaxation-optimized spectroscopy (TROSY) triple resonance and ^{1}H-^{15}N heteronuclear single quantum coherence (HSQC) experiments were used for backbone resonance assignment experiments and ligand titrations, respectively, as described in *SI Materials and Methods*.

Results

Generation and Characterization of Mixed Dimers. To study intersubunit communication in a homodimeric protein, we sought to use NMR to investigate the effect that binding of the first ligand has on both subunits of thymidylate synthase. Study of lig_1 states, however, requires overcoming two primary degeneracies. The first is that addition of ligand to populate the lig_1 state is typically accompanied by population of lig_0 and lig_2 states, and accordingly, more complex spectra. The second is that, for symmetric protein dimers, it can be difficult to spectroscopically distinguish between the bound and empty protomers (or subunits). Our strategy was to break these degeneracies by creation of mixed ^{15}N-labeled dimers that (*i*) can bind substrate only in one protomer, and (*ii*) have only a single protomer labeled for NMR detection, allowing for two complementary lig_1 dimer samples, one with the bound subunit ^{15}N-labeled and a second lig_1 sample with the empty subunit ^{15}N-labeled.

Mixed labeled dimers with a single functional active site were prepared by first abolishing substrate binding with an active site mutation (R126E, R127E). Mixing this inactive, purified homodimer with purified ^{15}N-labeled WT homodimer yielded three species, one of which is the mixed dimer with the nonfunctional subunit (the WT) ^{15}N-labeled (Fig. 1*A*) (note that the mutation at positions 126–127 abolishes binding to the opposite subunit because the loop bearing the arginine mutations forms critical

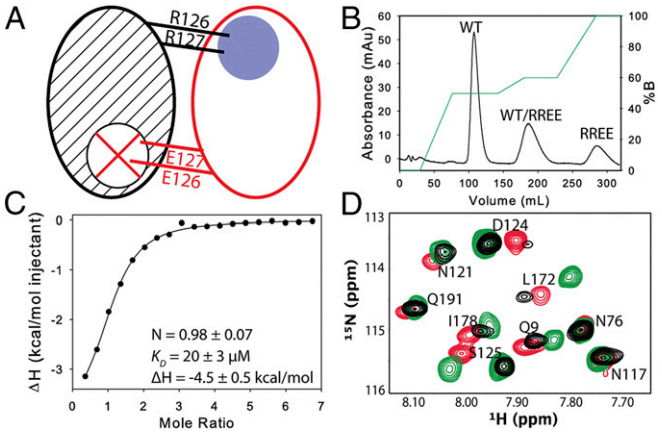

Fig. 1. Characterization of the mixed dimers. (*A*) Schematic of a mixed labeled dimer showing the sites of mutation. The WT subunit (black) is ^{15}N-labeled (hashed), and the RREE mutant subunit (red) is unlabeled. The blue circle and red X indicate the functional and nonfunctional binding site, respectively. (*B*) Chromatogram showing separation of the three species using anion exchange. (*C*) dUMP binding to the mixed dimer was measured by isothermal titration calorimetry (ITC); mean and SD are from three replicates. For the selected isotherm, mixed dimer concentration was 150 μM with 3 mM dUMP in the syringe. (*D*) Overlay of HSQC spectra of apo WT (black), WT-labeled (green), and RREE-labeled (red) mixed dimers. Residues proximal to the mutation are D124 and S125 in the RREE-labeled and L172 in the WT-labeled mixed dimers.

interactions with dUMP in the opposite subunit). Labeling of the functional subunit is achieved by ^{15}N-labeling the mutant enzyme and subsequent mixing with unlabeled WT (and purification from the two homodimers) (Fig. 1*B*). Binding of dUMP to the mixed dimer, measured by isothermal titration calorimetry (Fig. 1*C*), was similar to the WT (ΔH_1 of −4.5 kcal/mol, ΔH_2 of −4.4 kcal/mol and $K_{D1} = K_{D2}$ of 16 μM) (16). HSQCs of the apo mixed dimers showed that the mutation primarily affects nearby residues, with minimal effects on distal sites (Fig. 1*D*). With this pair of mixed labeled dimers, addition of dUMP yielded lig_1 samples with ^{15}N chemical shift probes distributed throughout the bound or empty subunit, enabling subunit-specific tracking of ligand-binding effects without interference from $dUMP_0$ or $dUMP_2$.

Imbalanced Chemical Shift Response to dUMP Binding. With the two mixed dimers, we characterized the subunit-specific effects of the first and second dUMP binding events using standard chemical shift perturbations (CSPs). ^{1}H-^{15}N CSPs due to the first dUMP binding event were calculated directly from the mixed labeled dimers to monitor perturbations in each subunit. The bound subunit of $dUMP_1$ showed large CSPs in the binding site, dropping off ∼20 Å from dUMP, with smaller perturbations extending along the interface, out to ∼28 Å from dUMP (Fig. 2*A*). The empty subunit was largely unaffected, dropping off ∼15 Å from dUMP, with all of the CSPs in the dUMP binding loop (residues 123′–128′, where prime indicates the empty subunit) and the backside of the binding site (residues 150′–163′) (Fig. 2*B*). Overall, the effects of binding the first dUMP were highly localized, primarily to the binding region, with small perturbations to the dimer interface (Fig. S1*A*).

Although CSPs for the second dUMP binding event ($dUMP_1$ to $dUMP_2$) cannot be directly calculated, they can be obtained indirectly from the mixed dimers by reconstructing the WT $dUMP_1$ chemical shifts, which was accomplished using a vector-based correction to account for the effects of the RREE mutation (Fig. 3 and *SI Materials and Methods*). This correction allows generation of WT $dUMP_1$ chemical shifts from the mixed dimer $dUMP_1$ chemical shifts (open circles in Figs. 3 and 4). The correction was cross-validated separately on a reference complex (Fig. S2 and *SI Materials and Methods*). In contrast to the first dUMP, the second

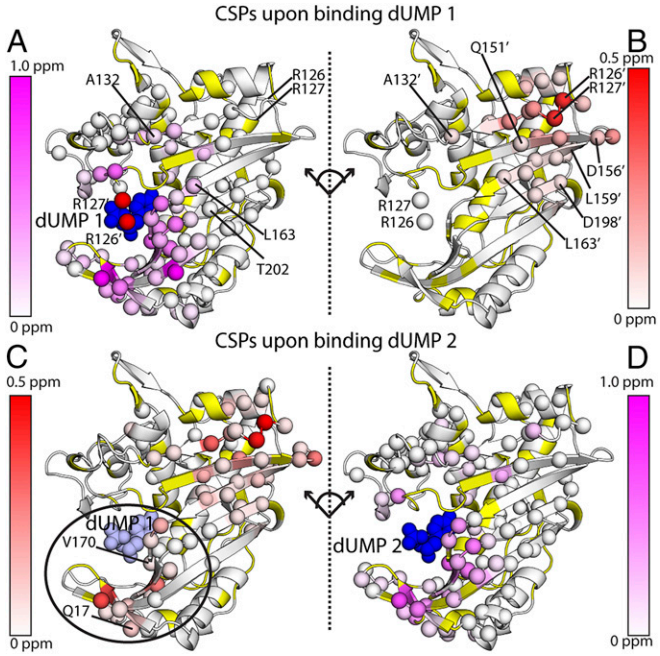

Fig. 2. Chemical shift perturbations of the two dUMP binding events. The effects of binding the first dUMP to the binding (*A*) and nonbinding (*B*) subunits of the dimer are shown at the *Top*, using the CSP scheme shown in Fig. 3*A*. The effects of binding the second dUMP to the nonbinding (*C*) and binding (*D*) subunits are shown at the *Bottom*, using the reconstructed WT CSPs shown in Fig. 3*B*. Viewing the dimer interface region is enhanced by separating the two subunits, where the subunits on the right underwent a hinge-type rotation (dotted line) to yield the same viewing angle as those on the left. As a reference point for the rotation, the red (*A*) and white (*B*) spheres show the locations of R126 and R127 from the other subunit. Residues with significant CSPs are shown as spheres. Residues that are missing or unassigned are in yellow. Annotated residues are discussed in Figs. 4 and 5, where residues denoted prime (e.g., R126′) correspond to the empty subunit of the $dUMP_1$ state. The first bound (dUMP 1) and second bound (dUMP 2) dUMPs are shown in dark blue; for binding of dUMP 2 (*Bottom*), the previously bound dUMP 1 is shown in light blue. In *C*, the circle highlights the major difference in the distant subunit response for binding of dUMP 1 and dUMP 2. The CSPs in context of the full dimer are shown in Fig. S1.

dUMP had more pronounced effects throughout the entire protein. The effects of the second dUMP on the binding subunit resembled the effects of the first dUMP, with the largest and majority of the perturbations localized around the binding site (Fig. 2*D*). Most notably, however, unlike the first dUMP, the second dUMP caused significant perturbations to the other binding site: in this case, the site bound by the first dUMP (e.g., Q17 and V170) (Fig. 2*C*). The widespread perturbations in both subunits upon the second binding dUMP indicated subunit communication between the two binding sites. Overall, the CSP analysis showed an imbalance in the subunits' responses to the two dUMP binding events: CSPs were limited to the binding site for the first dUMP but covered the interface and both binding sites for the second dUMP.

Ligand State Multiplets Reveal That $dUMP_1$ Is an Extreme State. Although standard CSP analysis is effective at revealing overall perturbations of large magnitude, it can also obscure, especially in the case of a homodimer, interesting chemical shift behavior. To view the complete WT chemical shift responses, we sought to visualize relative peak positions of the $dUMP_0$, $dUMP_1$ (reconstructed), and $dUMP_2$ states for each residue amide. In general, these overlays yielded four-peak ligand state multiplets (Fig. 4) because the $dUMP_0$ and $dUMP_2$ states yielded single peaks due to dimer symmetry, and the $dUMP_1$ state can yield two distinct peaks, one from each of the mixed dimer samples. For clarity, we used superscripts "apo," "empty," "bound," and "doub" to refer to peak positions of the $dUMP_0$ state, the empty subunit of the $dUMP_1$ state, the bound subunit of the $dUMP_1$ state, and the $dUMP_2$ state, respectively.

One interesting feature of the multiplets is that, in some cases, the peak positions of the $dUMP_1$ state actually extended further than the $dUMP_2$ peaks, which we refer to as "supershifting." Supershifting can be seen for V170 and Q17 (Fig. 4 *A* and *B*), where $V170^{bound}$ ($Q17^{bound}$) shifts in the same direction as $V170^{doub}$ ($Q17^{doub}$), but actually shifts beyond $V170^{doub}$ ($Q17^{doub}$). The simple case where supershifting is along the apo–doub chemical shift change vector suggests a fast equilibrium of free and bound states, and, oddly, binding the first dUMP pushes the equilibrium further than the second dUMP. Alternatively, it could suggest that protomers may not simply snap into a free or bound conformation, but rather that there are additional states that protomers can adopt and that binding the first dUMP induces a more extreme state. Much of the $dUMP_1$ supershifting occurs around the binding site (Fig. S3 *A* and *B*), which, remarkably, explains the long-range intersubunit communication observed upon binding the second dUMP (Fig. 2*C*). Because the first dUMP seems to induce an extreme state beyond what is observed in the $dUMP_2$ state, and one that cannot be supported with both subunits bound, a response is set up in which binding the second dUMP partially reverses the initial shift (e.g., V170 in Fig. 4*A*). This result leads to intersubunit communication upon binding the second dUMP by making corrections to supershifting caused by the first dUMP.

More complex shifting behavior was seen in additional residues. For example, A132 exhibited not only supershifting, but also an $A132^{empty}$ and $A132^{bound}$ shift in a direction orthogonal to the $A132^{apo}$–$A132^{doub}$ vector, termed "orthogonal shifting," indicating that such sites are not simply in a fast, two-state equilibrium (Fig. 4*C*). This result, again, points to the existence of an additional state that becomes significantly populated upon binding the first dUMP. Another multiplet pattern we observed was "reverse shifting," where $dUMP_1$ peaks shift in the opposite direction of the apo–doub chemical shift vector (Fig. 4 *D* and *E*). It is not immediately clear why reverse shifting was observed although, along with supershifting, it suggests that there are compensatory behaviors occurring in the protomers upon binding the first dUMP. Overall, the observations of supershifting, orthogonal shifting, and reverse shifting suggest that a single dUMP binding induces sampling of extreme conformations relative to apo and $dUMP_2$ states.

Using ligand state multiplets from spectral overlays to assess specific residue chemical shift behaviors is generally not practical because the four peaks from each residue render the spectra too crowded. Thus, to enhance the analysis of multiplet behavior, we

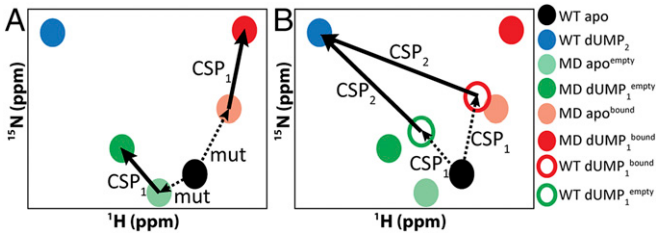

Fig. 3. Vector correction to determine WT $dUMP_1$ peak positions. The two schematic diagrams show how CSPs were calculated for each dUMP binding event (*SI Materials and Methods*). (*A*) The CSPs for binding the first dUMP, CSP_1, were calculated directly from the apo and $dUMP_1$ peak positions of the two mixed labeled dimer (MD) samples (thick arrows). Dashed arrows show the CSP due to the mutation (mut). (*B*) CSPs for binding the second dUMP, CSP_2, were calculated as the vectors connecting the WT $dUMP_2$ peak (in blue) and the $dUMP_1$ peaks for WT (empty red and green circles), which were reconstructed by applying the CSP_1 vectors to the apo WT peak (dashed arrows).

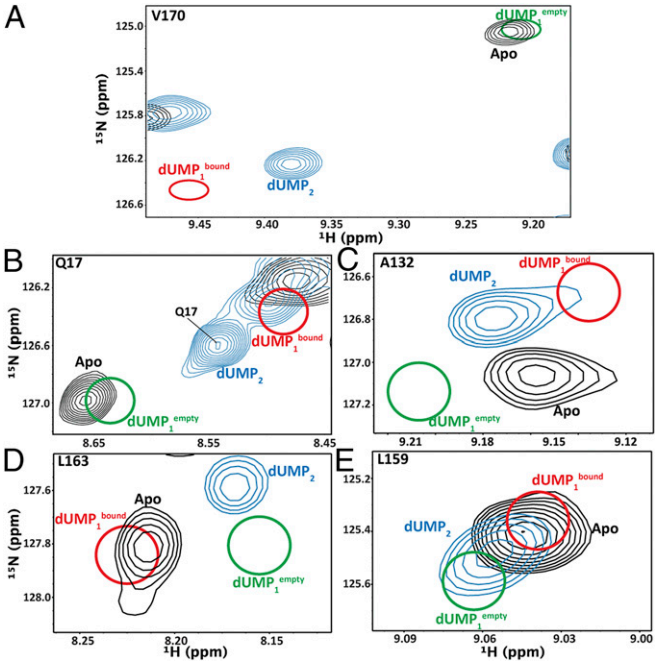

Fig. 4. dUMP ligand state multiplets. Spectral overlays of apo, $dUMP_1$, and $dUMP_2$ allow visualization of chemical shift behaviors. WT apo and $dUMP_2$ peaks are shown in black and blue, respectively. The WT $dUMP_1$ peaks reconstructed from the mixed dimer chemical shifts are shown as red (bound subunit) and green (empty subunit) circles. These panels show the three classes of extreme chemical shift behaviors of the $dUMP_1$ state. *A* and *B* highlight supershifting of $dUMP_1^{bound}$, *C* highlights orthogonal shifting, *D* highlights reverse shifting of $dUMP_1^{bound}$, and *E* highlights supershifting ($dUMP_1^{empty}$) coupled with reverse shifting ($dUMP_1^{bound}$).

condensed the information into "line plots" of ^1H and ^{15}N chemical shifts, which allowed for simpler viewing of chemical shifts to more conveniently inspect individual residues in terms of the spatial response to dUMP binding (Fig. 5 and Figs. S4 and S5). For simplicity, ^1H line plots are shown although corresponding ^{15}N line plots are also easily viewed (Fig. S4*B*). From the line plots, we identified clusters of residues with similar behaviors, indicating regions of ligand sensitivity throughout the protein. Residues 155, 156, and 195 (Fig. 5*A*) are spatially clustered and exhibit similar supershifting behavior, indicating an extreme state (or skewed population) in this region. In the case of E195, the two sites are nearly equidistant from dUMP, ~28 Å, yet $E195^{empty}$ supershifts and $E195^{bound}$ hardly shifts, showing how communication can be more effective across the interface. Residues in the central helix, in particular I178 and A179 (Fig. 5*B*), show that ligand binding can be sensed at distal sites even with no direct contact to, or across, the interface. Additionally, these regions show a symmetric pattern in which supershifting in one subunit is linked with reverse shifting in the other. This pattern was observed frequently throughout TS, indicating extensive compensatory behavior between subunits. Residues along the interface (Fig. 5*C*) showed the largest variety, as well as the most symmetric, of behaviors. These residues in particular reflect the quasi-symmetrical, compensatory shifts that occur where a partial shift or supershift in one subunit is coupled with a partial or reverse shift in the other subunit: e.g., V199, and D198. In summary, using mixed labeled dimers coupled with viewing ligand state multiplets via line plots facilitates thorough inspection of shifting from binding of both dUMP molecules, and extensive supershifting and reverse shifting indicate significant population of extreme states (or a further shifting of the equilibrium) beyond the known apo and $dUMP_2$ conformations.

Subunits' Response to Diligand Binding Is Equally Balanced. Although the mixed dimers are required to visualize the $dUMP_1$ states, they are not required for the cofactor binding step of the reaction. Binding of a substrate analog, 5-FdUMP, along with cofactor, together referred to as the "diligand," forms a covalent bond to the enzyme, leading to a stable ternary complex (22, 23). Because of the covalent nature of this complex, the resonances from the diligand-bound TS are in slow exchange, and, thus, the chemical shifts of the $diligand_1$ states can be more easily measured (*SI Materials and Methods*) (16). Together, dUMP and diligand will allow us to compare the proteins' response, not only to an additional binding event but also to a conformational change, because, unlike dUMP binding, diligand binding causes significant conformational changes in the vicinity of the binding site to form the closed ternary complex (22, 24).

CSP analysis highlighted a number of interesting differences between dUMP and diligand binding (Fig. 2 and Fig. S6). Binding of the first diligand had overall larger magnitude and more extensive CSPs in both the binding and empty subunits than did dUMP, likely due to the combined effects of the conformational change and increased size of the diligand relative to dUMP (Fig. S6 *A* and *B*). Most notably, the effects of the first diligand propagated further in both subunits, ~30 Å from diligand, extending almost all the way to the second binding site. Thus, unlike with dUMP binding, there was clearly communication between the two sites upon binding the first diligand. Additionally, similar to dUMP binding, the effects of the second diligand on the binding subunit resembled those of the first (Fig. S6*D*). Most strikingly, there were no significant perturbations to the other binding site, as with dUMP (Fig. S6*C*). Overall, the similarities in the CSPs for the two diligand binding events indicate a balanced response to diligand binding, in contrast to dUMP binding. This balanced response to diligand is also evident in the diligand line plots (Fig. S7). Not surprisingly, the diligand line plots show more symmetrical and fewer extreme features, with the vast

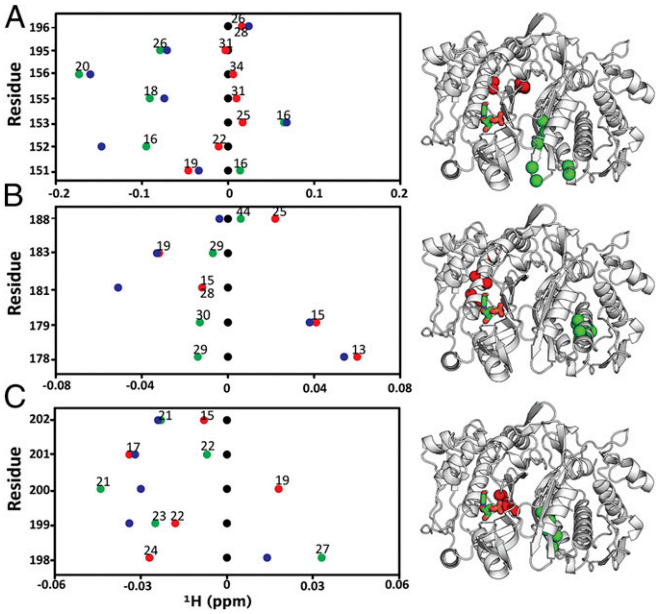

Fig. 5. Line plots of ^1H chemical shifts. These line plots show how the chemical shift behaviors observed from ligand state multiplets are distributed throughout the protein. ^1H chemical shift changes (relative to apo) are plotted for apo (black), $dUMP_2$ (blue), $dUMP_1^{bound}$ (red), and $dUMP_1^{empty}$ (green). Each of the $dUMP_1$ points is labeled with the distance (in Å) of that residue (red and green spheres) from the bound dUMP (sticks). Distances are measured from the amide N to the centroid of the bound dUMP. (*A*) Behaviors of residues at opposite ends of the dimer interface. (*B*) Behaviors of interior residues. (*C*) Behaviors of residues at the center of the dimer interface.

majority of the diligand$_1$ peaks either coinciding with, or being equally displaced from, the diligand$_0$ and diligand$_2$ peaks. Accordingly, there were very few diligand residues that showed supershifting (Fig. S3). However, as with dUMP, when supershifting did occur, it was often coupled with reverse shifting, yielding symmetrical patterns.

Discussion

In this study, we used mixed labeled dimers to investigate, by NMR, intersubunit signaling in response to single ligand (dUMP or diligand) binding events in the homodimeric enzyme thymidylate synthase (TS). The mixed dimer approach allows for isolation of singly ligated (lig$_1$) states and breaks the symmetry degeneracy in the NMR signals. This approach yields a rare example of step-wise progression of chemical shifts upon binding identical ligands in a homodimer and prompted the use of visualization strategies beyond simple CSPs. Standard CSP analysis revealed that only the binding of the second dUMP "signals" to the other binding site. This modulation of second ligand binding due to changes at the first site represents a nonintuitive yet valid potential allosteric mechanism. More generally, a distribution of ligand state peak multiplets were observed that point to regional behaviors, including the surprising observation of shifting of lig$_1$ peaks beyond lig$_2$ peaks, termed "supershifting" here. There was also a surprising degree of quasi-symmetrical responses in the two protomers, especially in the diligand complex, indicating substantial compensatory behavior coupled across the dimer interface. One caveat of the RREE mixed dimers used here is that, without binding of the second ligand, there can technically be no functional allostery. The primary goal, however, was to observe the mechanistic preparations that the homodimer makes before the second ligand binding event that enable the allosteric effect. Although the RREE mutation may have altered some of these preparations, the reconstructed binding steps yielded much useful information about allosteric communication. Although the focus of this study was on chemical shifts, clearly this strategy lends itself to protomer-specific NMR measurements, such as spin relaxation for the characterization of dynamics, on specific ligation states. Lastly, although the strategy used here applies primarily to tight dimers that do not readily dissociate, it can potentially be applied to other systems by covalently linking the monomers.

Insights into Allostery from Ligand State Peak Multiplets. The mixed labeled dimers allow for simple viewing of complete ligand state NMR peak multiplets, which, to our knowledge, have not been previously reported. The patterns observed in the multiplets can provide a format for evaluating allosteric models. For example, the most easily observed patterns are the doublets that would arise from a Koshland–Némethy–Filmer (KNF) or Monod–Wyman–Changeux (MWC) type system, and their expected intensities (12, 25), with only two possible states (Fig. 6 *A* and *B*). In the KNF system, where only the binding subunit responds to ligand, the lig$_1^{bound}$ and lig$_1^{empty}$ peaks would coincide with the lig$_2$ and lig$_0$ peaks, respectively. In the MWC system, ligand binding causes a concerted shift in both subunits, where both lig$_1$ peaks would coincide with the lig$_2$ peak. Alternatively, one might expect to observe two possible linear triplet patterns, one where one of the lig$_1$ peaks coincides with either the lig$_2$ or lig$_0$ peaks and the other is partially shifted toward lig$_2$, or one where both lig$_1$ peaks are partially shifted toward lig$_2$ (Fig. 6 *C* and *D*) (12). We observed such triplet patterns in our dUMP data as did others previously in studies of half-titrated, negatively cooperative dimers that are in the slow exchange regime (12, 26). Interestingly, we also observed many nonlinear triplets, and quartets (Fig. 6 *E* and *G*), that indicate behaviors beyond simple population or exchange between lig$_0$ and lig$_2$ states. It is currently not clear precisely what structural changes produce these nonlinear multiplets although it must involve at least a third conformation distinct from the lig$_0$ and lig$_2$ conformations. Given this diverse set of multiplet patterns, it seems that there is not a consistent response throughout the protein, but, rather, TS has a mixture of intersubunit responses to binding of dUMP. Evaluation of the ligand state multiplets makes this response clear, and it is possible to do so outside of the slow exchange condition. In general, the evaluation of NMR ligand state multiplets in oligomeric proteins is a powerful approach to characterize allosteric mechanisms in proteins (12, 25).

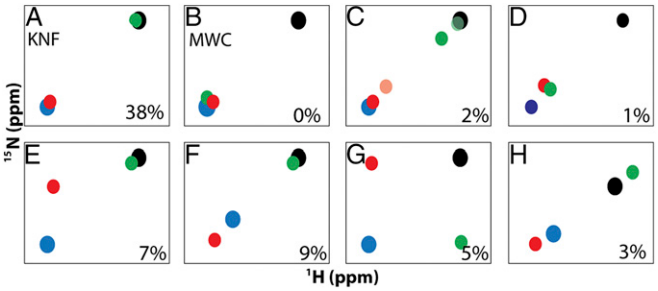

Fig. 6. Observable patterns for ligand state multiplets. Schematic HSQC peak patterns according to allosteric model (*A* and *B*) or observed for dUMP binding in TS as resolved triplets (*C*–*F*) or quartets (*G* and *H*). Peaks are shown for apo/lig$_0$ (black), lig$_1^{bound}$ (red), lig$_1^{empty}$ (green), and lig$_2$ (blue). In *C*, two partial shifting behaviors are shown in which lig$_1$ partial peak shifting is observed in the binding subunit (light red) or in the empty subunit (dark green). Behaviors are observed for supershifting (*F*), orthogonal shifting (*G*), and reverse shifting (*H*). In each panel, the percentages indicate the abundance of the peak pattern for dUMP binding to TS.

Perhaps the most surprising multiplet pattern evident was the observation of supershifting (and reverse shifting) in the lig$_1$ state, which was unexpected under the assumption that lig$_0$ and lig$_2$ peak positions represent end states. However, as is apparent here and from previous studies (27, 28), this assumption is not always a good one because peak positions of specific mutants point to a shift in the equilibrium beyond the assumed end points of apo and ligand bound, which suggests that, for those sites, the apo and ligand saturated states (29) both represent dynamic equilibria between two extreme states that are not readily detected. It is interesting that, although supershifting and reverse shifting have been observed from comparisons of mutant and WT peak positions, here they are observed from lig$_1$ peak positions. It is also interesting that these behaviors are highly dependent on the residue (Fig. S3). Although changes in two-state equilibria can explain NMR peaks moving in a linear fashion, they cannot explain orthogonal peak movement. Therefore, a general explanation for the various behaviors observed here is that the lig$_1$ state peak positions may reflect a range of different local conformations that TS samples upon binding the first ligand. These conformations may represent different sets of interactions (hydrogen bond geometries, for example) that lead to particular lig$_1$ chemical shifts. Thus, TS may reside in a relatively shallow conformational basin on the energy landscape that allows it to modulate various interactions by conformational adjustment, yielding different chemical shifts, upon binding one or two ligands. This scenario provides a more flexible model for interpreting chemical shifts and is fundamentally distinct from two-state switching.

Lig$_1$ Asymmetry from X-Ray and NMR Chemical Shifts. Although the functional significance of these multiplet behaviors remains to be determined, there is a precedent for the asymmetric effects of dUMP binding to TS. A crystal structure of *Pneumocystis carinii* TS bound to dUMP and a cofactor analog, CB3717, has an asymmetric ternary complex wherein one active site has both dUMP and cofactor bound whereas the other has only dUMP bound (17). A key observation from this structure is that, in addition to the global changes that occur upon cofactor binding, there are subtle, yet significant conformational differences between the two monomers for a number of residues along the otherwise rigid dimer interface. It was proposed that these

residues are the primary candidates for signaling between the active sites and could provide the basis for cooperativity. Of these residues, 75% exhibited nonlinear or supershifted triplets and quartets here for dUMP binding. The fact that we see such extensive overlap could suggest that these subtle structural rearrangements are also occurring in the $dUMP_1$ state. The nonlinear shifts observed for these residues point to an additional state outside the apo-bound equilibrium, rather than simply an equilibrium shift. This extreme state could be due to strain induced by binding the first dUMP, leading to an asymmetric lig_1 state. This strained conformational state may be the result of differential perturbations to the hydrogen-bonding network across the interface or to differences in dynamics between the two subunits in the lig_1 state. The fact that we see nonlinear behavior for these residues suggests that, if in fact these residues form a communication pathway, this extreme state may be one that is involved in TS cooperativity.

Given the long-range, intersubunit impact of binding the second dUMP, it is surprising that dUMP binding is thermodynamically noncooperative at 25 °C, at which the NMR chemical shifts were investigated. However, at lower temperatures, the $\Delta H°_{bind}$ values for the first and second dUMP molecules are nonequivalent, reflecting intrinsically different $\Delta C_p°$ values for the two binding events. Thus, the underlying thermodynamics can be considered nonidentical for the two binding events, which could be reflected in the observed chemical shift behaviors. Furthermore, although dUMP binding does not trigger functional intersubunit allostery, it may still reveal the intrinsic communication mechanisms that could potentially lead to functional allostery during subsequent reaction steps. Overall, the presence of communication upon dUMP binding could indicate that TS is poised for intersubunit allostery.

Potential Origin of Symmetrical Chemical Shift Response. Based on the observations made here, we propose that binding of the first dUMP or diligand to the structurally symmetric dimer imparts compensatory effects between the two protomers. In the case of dUMP binding, presuming there is no significant conformational change, the symmetrical chemical shift changes arise from either propagation of changes in hydrogen bonding strengths in a symmetrical fashion, or from compensatory dynamical responses between the two protomers, or a combination of both. In the case of diligand binding, given that there is likely a conformational change in the bound subunit (22, 24), the symmetrical chemical shift changes are even more surprising because the shift in the bound subunit from the structural change cannot be replicated in the empty subunit. In either case, the propagation of chemical shift changes likely represents a form of structural or dynamic strain that, remarkably, has opposite manifestations in the two protomers for many residues. These considerations of quasi-symmetrical multiplets provide a unique view into how intersubunit allostery can be achieved for the simple example of symmetric homodimers. It seems that, at least for TS, symmetric cross-dimer interactions are "built in," such that quasi-symmetrical strain is introduced by the binding of the first ligand. The magnitude of symmetric chemical shift multiplet patterns and their extent throughout the protein indicate that TS is incredibly sensitive to substrate binding at sites throughout its structure, but particularly at the dimer interface. A fundamental question for understanding allostery is whether the intrinsic compensatory effects observed here will be observed in other homodimeric proteins, especially those that are allosteric with regard to binding two ligands.

ACKNOWLEDGMENTS. This work was supported by National Institutes of Health Grant GM083059 (to A.L.L.).

1. Cui Q, Karplus M (2008) Allostery and cooperativity revisited. *Protein Sci* 17(8): 1295–1307.
2. Lisi GP, Loria JP (2016) Solution NMR spectroscopy for the study of enzyme allostery. *Chem Rev* 116(11):6323–6369.
3. Nussinov R, Tsai CJ (2015) Allostery without a conformational change? Revisiting the paradigm. *Curr Opin Struct Biol* 30:17–24.
4. Tsai CJ, Del Sol A, Nussinov R (2009) Protein allostery, signal transmission and dynamics: A classification scheme of allosteric mechanisms. *Mol Biosyst* 5(3):207–216.
5. Klemm JD, Schreiber SL, Crabtree GR (1998) Dimerization as a regulatory mechanism in signal transduction. *Annu Rev Immunol* 16:569–592.
6. Lipchock JM, Loria JP (2010) Nanometer propagation of millisecond motions in V-type allostery. *Structure* 18(12):1596–1607.
7. Zhuravleva A, Clerico EM, Gierasch LM (2012) An interdomain energetic tug-of-war creates the allosterically active state in Hsp70 molecular chaperones. *Cell* 151(6):1296–1307.
8. Akimoto M, et al. (2015) Mapping the free energy landscape of PKA inhibition and activation: A double-conformational selection model for the tandem cAMP-binding domains of PKA RIα. *PLoS Biol* 13(11):e1002305.
9. Williamson MP (2013) Using chemical shift perturbation to characterise ligand binding. *Prog Nucl Magn Reson Spectrosc* 73:1–16.
10. Selvaratnam R, Chowdhury S, VanSchouwen B, Melacini G (2011) Mapping allostery through the covariance analysis of NMR chemical shifts. *Proc Natl Acad Sci USA* 108(15):6133–6138.
11. Popovych N, Sun S, Ebright RH, Kalodimos CG (2006) Dynamically driven protein allostery. *Nat Struct Mol Biol* 13(9):831–838.
12. Stevens SY, Sanker S, Kent C, Zuiderweg ER (2001) Delineation of the allosteric mechanism of a cytidylyltransferase exhibiting negative cooperativity. *Nat Struct Biol* 8(11):947–952.
13. Johnson EF, Hinz W, Atreya CE, Maley F, Anderson KS (2002) Mechanistic characterization of Toxoplasma gondii thymidylate synthase (TS-DHFR)-dihydrofolate reductase: Evidence for a TS intermediate and TS half-sites reactivity. *J Biol Chem* 277(45):43126–43136.
14. Maley F, Pedersen-Lane J, Changchien L (1995) Complete restoration of activity to inactive mutants of Escherichia coli thymidylate synthase: Evidence that E. coli thymidylate synthase is a half-the-sites activity enzyme. *Biochemistry* 34(5):1469–1474.
15. Saxl RL, Changchien LM, Hardy LW, Maley F (2001) Parameters affecting the restoration of activity to inactive mutants of thymidylate synthase via subunit exchange: Further evidence that thymidylate synthase is a half-of-the-sites activity enzyme. *Biochemistry* 40(17):5275–5282.
16. Sapienza PJ, Falk BT, Lee AL (2015) Bacterial thymidylate synthase binds two molecules of substrate and cofactor without cooperativity. *J Am Chem Soc* 137(45):14260–14263.
17. Anderson AC, O'Neil RH, DeLano WL, Stroud RM (1999) The structural mechanism for half-the-sites reactivity in an enzyme, thymidylate synthase, involves a relay of changes between subunits. *Biochemistry* 38(42):13829–13836.
18. Dev IK, et al. (1994) Mode of binding of folate analogs to thymidylate synthase: Evidence for two asymmetric but interactive substrate binding sites. *J Biol Chem* 269(3): 1873–1882.
19. Lovelace LL, Gibson LM, Lebioda L (2007) Cooperative inhibition of human thymidylate synthase by mixtures of active site binding and allosteric inhibitors. *Biochemistry* 46(10): 2823–2830.
20. Reilly RT, Barbour KW, Dunlap RB, Berger FG (1995) Biphasic binding of 5-fluoro-2′-deoxyuridylate to human thymidylate synthase. *Mol Pharmacol* 48(1):72–79.
21. Swiniarska M, et al. (2010) Segmental motions of rat thymidylate synthase leading to half-the-sites behavior. *Biopolymers* 93(6):549–559.
22. Hyatt DC, Maley F, Montfort WR (1997) Use of strain in a stereospecific catalytic mechanism: Crystal structures of Escherichia coli thymidylate synthase bound to FdUMP and methylenetetrahydrofolate. *Biochemistry* 36(15):4585–4594.
23. Santi DV, McHenry CS, Perriard ER (1974) A filter assay for thymidylate synthetase using 5-fluoro-2′-deoxyuridylate as an active site titrant. *Biochemistry* 13(3):467–470.
24. Stroud RM, Finer-Moore JS (2003) Conformational dynamics along an enzymatic reaction pathway: Thymidylate synthase, "the movie". *Biochemistry* 42(2):239–247.
25. Freiburger LA, et al. (2011) Competing allosteric mechanisms modulate substrate binding in a dimeric enzyme. *Nat Struct Mol Biol* 18(3):288–294.
26. Tzeng SR, Kalodimos CG (2009) Dynamic activation of an allosteric regulatory protein. *Nature* 462(7271):368–372.
27. Gardino AK, et al. (2009) Transient non-native hydrogen bonds promote activation of a signaling protein. *Cell* 139(6):1109–1118.
28. McDonald LR, Boyer JA, Lee AL (2012) Segmental motions, not a two-state concerted switch, underlie allostery in CheY. *Structure* 20(8):1363–1373.
29. Beach H, Cole R, Gill ML, Loria JP (2005) Conservation of mus-ms enzyme motions in the apo- and substrate-mimicked state. *J Am Chem Soc* 127(25):9167–9176.
30. Changchien LM, et al. (2000) High-level expression of Escherichia coli and Bacillus subtilis thymidylate synthases. *Protein Expr Purif* 19(2):265–270.
31. Agrawal N, Hong B, Mihai C, Kohen A (2004) Vibrationally enhanced hydrogen tunneling in the Escherichia coli thymidylate synthase catalyzed reaction. *Biochemistry* 43(7): 1998–2006.
32. Hardy LW, Pacitti DF, Nalivaika E (1994) Use of a purified heterodimer to test negative cooperativity as the basis of substrate inactivation of Escherichia coli thymidylate synthase (Asn177–>Asp). *Structure* 2(9):833–838.
33. Kang X, Frey DD (2003) High-performance cation-exchange chromatofocusing of proteins. *J Chromatogr A* 991(1):117–128.
34. Schmidt M, Hafner M, Frech C (2014) Modeling of salt and pH gradient elution in ion-exchange chromatography. *J Sep Sci* 37(1-2):5–13.
35. Sapienza PJ, Lee AL (2014) Backbone and ILV methyl resonance assignments of E. coli thymidylate synthase bound to cofactor and a nucleotide analogue. *Biomol NMR Assign* 8(1):195–199.